



OPEN

## Surface properties of alkylsilane treated date palm fiber

Helanka J. Perera<sup>1✉</sup>, Anjali Goyal<sup>2</sup> & Saeed M. Alhassan<sup>2</sup>

The present work focuses on investigating the effect of *non-fluoro short-chain alkylsilane* treatment on the surface characteristic of date palm (*Phoenix dactylifera*) fiber. Raw date palm fiber (DPF) was treated with octylsilane and the surface properties of treated fiber was investigated using thermogravimetric analysis (TGA), fourier transform infrared (FTIR) spectroscopy, scanning electron microscopy (SEM), contact angle analysis and X-ray diffraction (XRD) on configuring the thermal stability, chemical structures and surface properties (morphology, hydrophobicity and crystallinity). The decomposition temperature of 75% mass loss raw and treated DPF, the onset of temperatures were increased from 464 to 560 °C with the introduction of alkylsilane. Hydrophobicity and crystallinity index of the DPF fibers were increased from 66.8° to 116° and 31 to 41, introducing octylsilane to raw DPF. The SEM and XRD experimental results showed that the octylsilane treatment could effectively increase the pore size and crystallinity index as an indication of the removal of non-crystalline cellulosic materials from DPFs. Thermal stability, hydrophobicity and crystallinity of the fibers increased on DPF after alkylsilane treatment. The results indicated that alkylsilane-treated DPFs were a suitable reinforcing substitute for hydrophobic polymer composite.

Over the past decades, polymer composites incorporated natural renewable fiber materials have taken the attention of researchers due to their lightweight (which makes composites lighter), low cost, bio-renewable character, biodegradable and resistant to deforestation<sup>1–3</sup>. Many studies have demonstrated that natural fibers have replaced conventional synthetic fibers as reinforcing material on polymer composites<sup>1–8</sup>. Many literature studies were carried out on different plant fibers, including cotton, rice husk, wheat straw, oil palm, bagasse jute, coir and date palm<sup>7,8</sup>.

In Gulf countries, the date palm is one of the most widespread plants among all other trees. The United Arab Emirates (UAE) is home to the most date palms globally. It is said to have 40 million date palm trees and at least 200 cultivars, 68 of which are commercially valuable<sup>9</sup>. The UAE has 16,342,190 productive date palms in 2006, which produced 757,600 tons of dates<sup>10</sup>. The United Arab Emirates was just named the world's leading date palm cultivator, with 42 million trees, as revealed on March 15, 2009. Due to the more considerable amount of date palm production, a significant amount of waste is generated annually and burned directly in an open field, which causes damage to the environment and humans. Considering all problems caused by waste materials can be used as renewable materials for economically valuable product synthesis, such as crates, basketry, rope and furniture. Last decade, date palm fiber (DPF) as a reinforcing agent on polymer composite is one of the interesting topics in research<sup>11–14</sup>. However, several downsides were questioned while using these natural plant fibers as a reinforcing material. Due to the water absorption tendency, poor compatibility between hydrophobic matrix and fibers is considered the leading cause because of three main plant fiber components: cellulose, hemicellulose and lignin, which are responsible for the hydrophilicity in the fibers. But this drawback can be suppressed by modification of fiber surface through chemical treatment that switchover to hydrophobic behaviors and promote adhesion between polymeric matrix and reinforcing materials<sup>15</sup>.

According to the literature, numerous ways have been investigated for surface modification of fibers<sup>16,17</sup>, with alkali<sup>18</sup>, silane<sup>19,20</sup>, water-repelling agents<sup>21</sup> and peroxide treatment<sup>22</sup> being a couple of treatment methods to modify the natural fibers. However, the silanization method is one of the more effective chemical methods for introducing surface hydrophobicity<sup>23–25</sup>. Research carried out by Mukhtar et al.<sup>26</sup> reported the impact of alkali and sodium carbonates used to treat the sugar palm fibers enhanced crystallinity, thermal stability and surface roughness compared to untreated fibers. Moreover, surface modification for DPFs carried out by Elbadry et al.<sup>16</sup> by using heat and chemical treatment in the furnace at 100 °C for 1 h and 1% NaOH at 100 °C for 1 h, respectively, able to clean the wax and fatty substances on fiber surface while leading on the improved mechanical performance of fibers. The optimal alkali concentration for surface treatment of DPF study carried out by Oushabi et al.<sup>11</sup>

<sup>1</sup>Maths and Natural Science, Abu Dhabi Women's Campus, Higher Colleges of Technology, Abu Dhabi, United Arab Emirates. <sup>2</sup>Department of Chemical Engineering, Khalifa University, PO Box 127788, Abu Dhabi, United Arab Emirates. ✉email: hperera@hct.ac.ae



**Figure 1.** (A) DPF tree, (B) DPF meshes from date palm tree.

reported usage of 5% NaOH in an aqueous solution enhances the thermal resistance of fibers and interfacial properties between interfacial properties fibers and polyurethane matrix. The same group<sup>12</sup> extended their work with 5% NaOH treated DPFs further modified with silane coupling agents (3-mercaptopropyltrimethoxysilane and 3-aminopropyltrimethoxysilane) in various concentrations to improve interface bonding between the fibers and the matrix. In a similar trend for surface modification of DPFs, Perera et al.<sup>19</sup>, our recent published work, highlight a comparison of fluoro and non-fluorosilane coupling agents on improvements in the structural and thermal properties of raw DPF liquid phase silanization technique.

In this study, DPFs were chemically treated in the presence of non-fluoro short-chain alkyl silane (octyltrichlorosilane) to create a hydrophobic surface to assess their feasibility as a polymer composite reinforcing material. Fourier transform infrared spectroscopy (FTIR), scanning electron microscope (SEM), thermal gravimetric analysis (TGA), contact angle and X-ray diffraction (XRD) analysis were used to investigate the chemical structure, morphology and physical properties (thermal, hydrophobicity and crystallinity) of raw and treated DPFs. This study aims to provide a systematic overview of how non-fluoro short-chain alkylsilane can be used to alter the surface and thermal properties of DPF.

## Experimental section

**Materials.** Octyltrichlorosilane (C8) was obtained from SigmaAldrich (St. Louis, MO, USA). Hexane was from Pharmco-Aaper (Brookfield, CT, USA). All chemicals were used as received. The raw date palm fiber (*Phoenix dactylifera*) meshes were collected from the Abu Dhabi Campus from Abu Dhabi, UAE (Fig. 1A). Date palm meshes were removed from the stem and sealed in polyethylene bags until the experiments were conducted (Fig. 1B). These DPF meshes were manually separated into single fibers and washed with distilled water to remove dust particles, sand and impurities. Cleaned fibers were dry for 24 h at room temperature.

## Methods

**Preparation of the treated date palm fibers.** DPF (1 g) was cleaned and reacted with 1 g of C8 in glass vials with 250 mL of hexane to cover the DPF completely. The silane reaction was carried out in a shaker for 4 h at 50 °C and 200 rpm. After shaking, treated DPFs were rinsed three times with 100 mL hexane to remove the unreacted C8 coupling agent. After that, the materials were maintained at room temperature until the characterizations were performed. All the plant experiments were in compliance with relevant institutional, national and international guidelines and legislation.

**Measurements and characterization.** *Thermo-gravimetric analysis (TGA).* TGA was performed to identify the degradation characteristics of the C8 treated fiber with the raw DPF. Hereafter, the grafted amount of C8 on the treated DPF was quantified using a TA Instruments, Model SDT 650 Thermogravimetric Analyzer (TA Instruments, New Castle, DE, USA). The treated DPF and raw DPF samples were heated from 20 to 900 °C with a heating rate of 20 °C/min in high purity nitrogen gas. The TGA thermograms were measured by running three samples from three different places of the untreated/treated DPF samples.

*Fourier transform infrared (FTIR) spectroscopy.* FTIR spectra were taken using a Perkin Elmer Frontier FTIR spectrometer (PerkinElmer Genetics Inc., Waltham, MA, USA). The scanning range was from 600 to 4000  $\text{cm}^{-1}$  with a spectral resolution of 4  $\text{cm}^{-1}$  and 32 scans. The three samples from three different places of the raw/treated DPF samples were run during FTIR analysis.



**Figure 2.** Fiber arrangement on a glass slide for contact angle measurement.

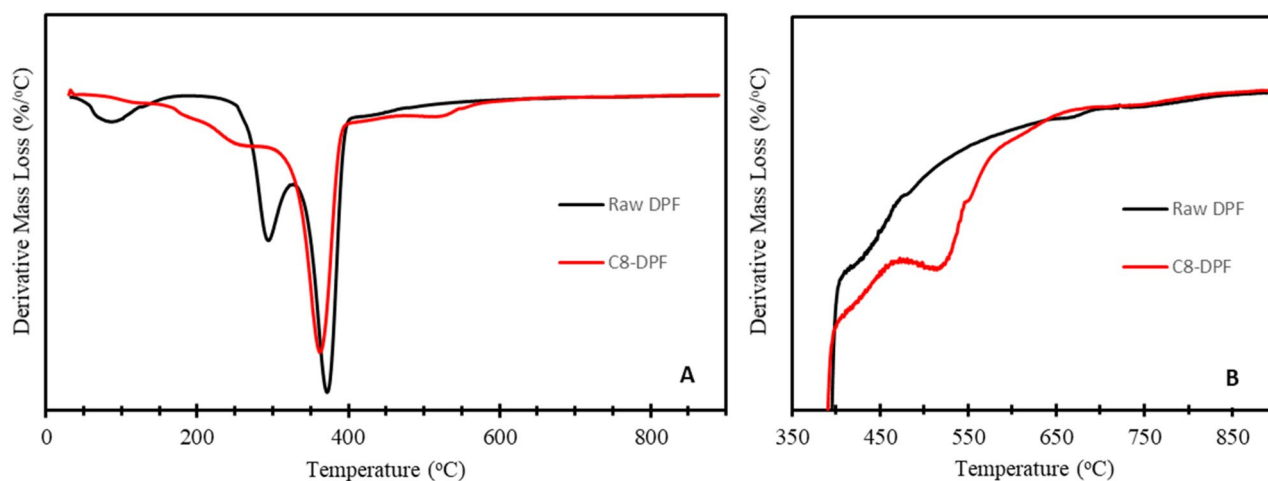


**Figure 3.** DTGA thermograms of raw DPF and C8-DPF.

**Scanning electron microscopy (SEM).** The surface morphology was carried out by scanning electron microscopy (SEM) using FEG Quanta 250 (FEI Company, Hillsboro, OR, USA) instrument of the raw and C8 treated DPFs under high vacuum mode operated at an acceleration voltage of 5 kV a working distance of about 10 mm. For SEM studies, each sample was attached to double-sided carbon adhesive tape on the top of an aluminum stud. The samples were then made conductive by the sputtering of Au/Pd.

**Contact angle analysis.** For contact angle measurements, the raw and C8 treated DPF samples were prepared on a glass slide by placing fibers close to each other with the help of double-sided sticky tape, as shown in Fig. 2. Water contact angle measurements were then performed using the static drop method at room temperature using KRÜSS DSA25 Series (KRÜSS Scientific Instruments, Inc., Matthews, NC, USA). Deionized water was used as a probe liquid (0.3  $\mu$ l dispense volume) at a frequency of 20 in a time interval of 3000 ms. Ten images from different locations on the surface were taken for each sample, with the average reported for the contact angle.

**X-ray diffraction (XRD).** Diffraction (XRD) patterns were collected using X'Pert PRO powder diffractometer (Cu-K $\alpha$  radiation 1.5406 Å, 45 kV, 40 mA) in the range of 5°–80°, 2 $\theta$  scale. The empirical method was used to obtain the crystallinity index (CI) of the samples<sup>27</sup>, as shown in Eq. (1):

$$CI = \left( \frac{I_{cr} - I_{am}}{I_{cr}} \right) \times 100 \quad (1)$$

where  $I_{cr}$  and  $I_{am}$  represent the crystalline intensity and amorphous intensity at an angle (2 $\theta$ ).  $I_{cr}$  is the crystalline peak corresponding to the intensity of approximately 23° and  $I_{am}$  is the amorphous peak corresponding to the intensity of approximately 19°. The XRD curves were measured by running three samples from three different places of the untreated/treated DPF samples.

## Results and discussion

**Thermogravimetric analysis (TGA).** The TGA thermograms for raw and C8 treated DPF samples are shown in Fig. 3. To more clearly show the nature of thermal degradation, the first derivative of mass losses are plotted against temperature. Figure 3A, the derivative curves of raw DPF and C8 treated DPF, showed three

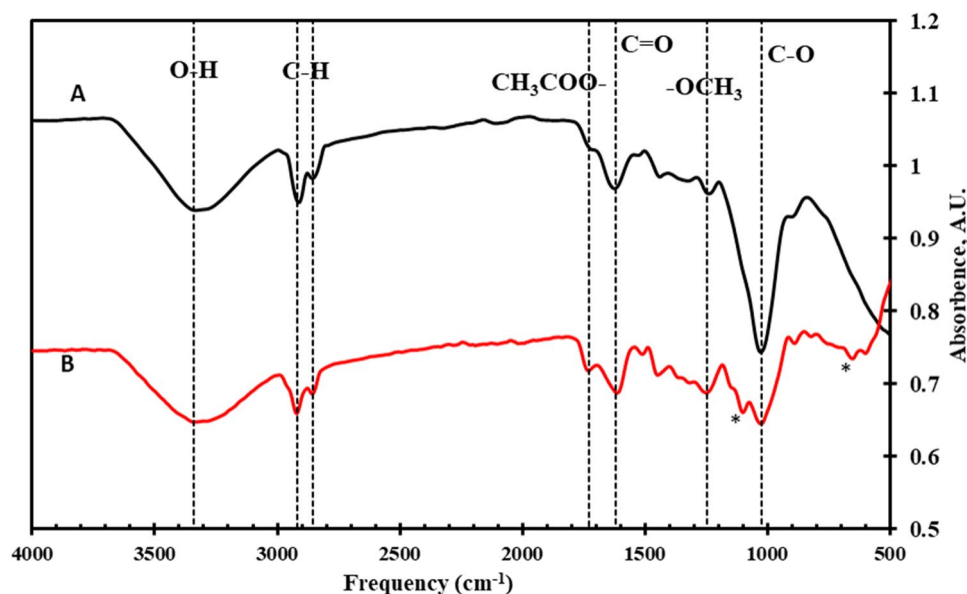


**Figure 4.** FTIR spectra for (A) raw DPF and (B) C8-DPF. Additional peaks appear after the C8 modification indicated with the \* symbol.

major mass losses in the temperature range of 25–400 °C. The first mass loss was associated with the removal of physically adsorbed water. The other two major degradations occur between 200 and 400 °C, related to the degradation of hemicellulose and lignin<sup>28,29</sup>. After modification of C8 on DPF, a decrease in mass losses of hemicellulose and lignin were observed on the C8-DPF compared to raw DPF. It indicates C8 silane treatment can remove hemicellulose and lignin or non-crystalline cellulose present in the fiber<sup>30</sup>. A significant broad mass loss occurred between 375 and 750 °C in raw and C8 treated DPF, as shown in Fig. 3B. For raw DPF, this broad mass loss was attributed to the degradation of cellulosic and other non-cellulosic materials present in the DPF<sup>28,29</sup>. The decomposition of C8-DPF gave a well-resolved peak around 520 °C, in addition to the broad mass loss, as shown in Fig. 3B. According to the literature, the pronounced mass loss in the temperature range 450–600 °C was attributed to the decomposition of the hydrocarbon chain of C8<sup>31</sup>. TGA thermograms confirm raw DPFs were successfully modified with the C8 silane coupling agent.

**Fourier transform infrared (FTIR) spectroscopy.** The structural changes in the fiber surface before and after treatment were investigated using FTIR spectroscopy to establish the chemical efficiency of silane treatments. FTIR spectra of the raw and C8-DPF are shown in Fig. 4. The common peak positions for raw and C8-DPF are indicated with the dotted line. The broad peak ranging from 3660 to 2990  $\text{cm}^{-1}$  was because of hydroxyl groups stretching vibration present in cellulose, hemicellulose, and lignin. The vibration peaks at 2919  $\text{cm}^{-1}$  and 2854  $\text{cm}^{-1}$  revealed asymmetric and symmetric  $\text{CH}_2$  stretching in cellulose/hemicellulose, respectively. The peaks at 1730  $\text{cm}^{-1}$ , 1620  $\text{cm}^{-1}$ , 1245  $\text{cm}^{-1}$  and 1023  $\text{cm}^{-1}$  are corresponded to ester carbonyl group stretching, C=O stretching in carboxylic acid in hemicellulose, O-CH<sub>3</sub> stretching in lignin and C–O stretching vibration, respectively, for both raw and C8-DPF<sup>11,12,32</sup>. After C8 silane treatment, new absorption bands are appeared in the region, between 1200 to 500  $\text{cm}^{-1}$ , which are specific for silane coupling agents. Indeed, two new bands emerge at 1100  $\text{cm}^{-1}$  and 670  $\text{cm}^{-1}$ , which are caused mainly by the vibration of Si–O–cellulose and Si–O–Si on the fiber, which is shown in Fig. 4 shows the \* symbol<sup>12,33,34</sup>. The FTIR results demonstrated that the C8 silane coupling agent chemically treats raw DPF surfaces.

**Scanning electron microscopy (SEM).** SEM is a powerful tool for studying the surface morphology of fibers. Figure 5 shows the relevant SEM images of the raw and C8 modified DPF. Figure 5A,B show the SEM images of the longitudinal surface of raw and C8-DPF. DPF has a cylindrical shape both with and without treatment, as shown in Fig. 5A,B. Silane treatment did not damage the shape of the fiber. When comparing raw DPF to C8 treated fiber, the diameter of the silane treated fiber is smaller. The removal of hemicellulose and lignin from the fibers causes the diameter to shrink. The findings are consistent with recent experimental data on oil palm fiber by Yousif et al.<sup>35</sup>, kenaf fiber by Chin and Yousif et al.<sup>36</sup> and hemp fiber by Sawpan et al.<sup>37</sup>. As illustrated in Fig. 5A,B, the raw DPF surface seems rougher, whereas C8-DPF appears to develop a smoother surface due to the filling up of the spaces by silane treatment. Figure 5C,D show SEM micrographs of raw and C8-DPF in the cross sections, respectively. With C8 treatment, fiber pores are increased due to the removal of hemicellulose and lignin.

**Contact angle analysis.** Hydrophobicity of the surface was measured using contact angle measurements. Water contact angles of raw and C8 treated DPF are shown in Fig. 6. The raw DPF had a contact angle of

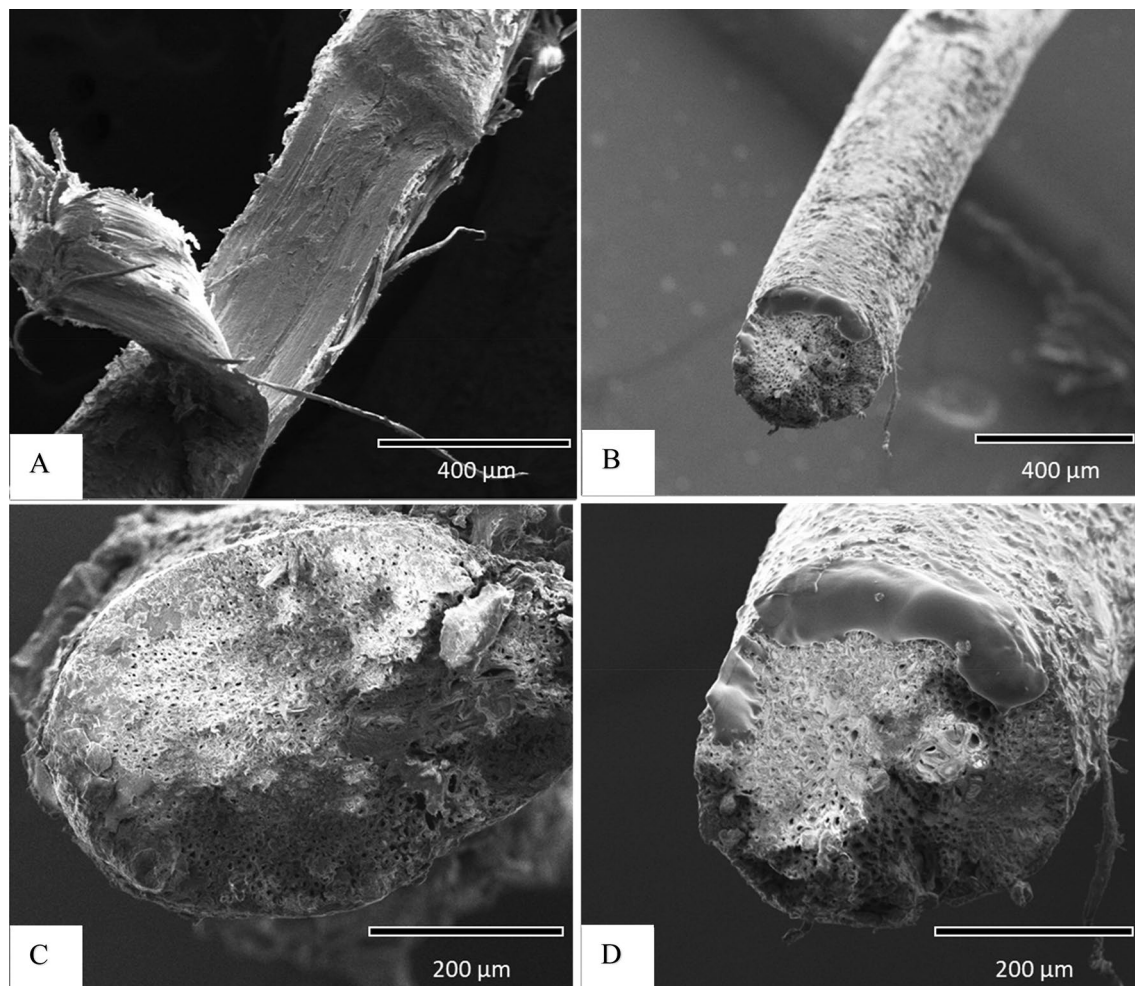


**Figure 5.** SEM of the longitudinal surfaces of (A) raw DPF and (B) C8-DPF, the cross sections of (C) raw DPF and (D) C8-DPF.

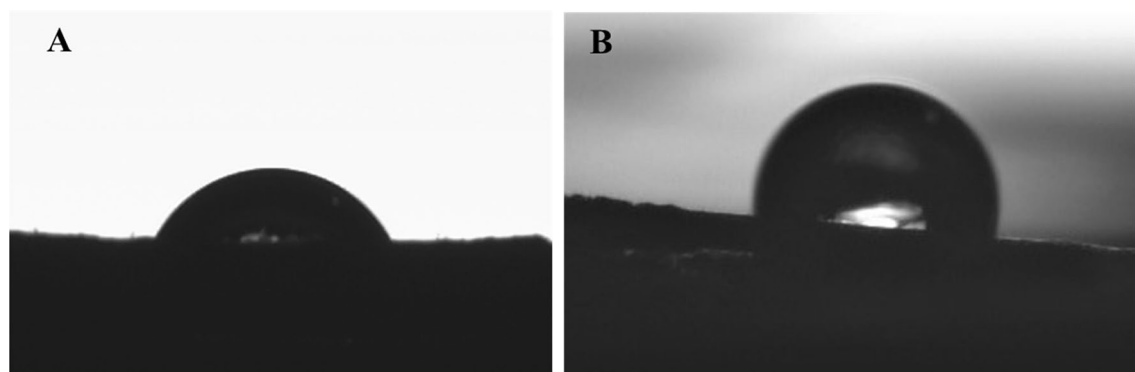


**Figure 6.** The contact angles of (A) raw DPF and (B) C8-DPF.

$66.8^\circ \pm 3^\circ$ . Free hydroxyl groups present on hemicellulose and lignin makes raw DPF hydrophilic<sup>38</sup>. The hydrophobicity of the raw DPF was enhanced to  $116^\circ \pm 24^\circ$  with modification of the DPF with the C8 silane coupling agent. Introducing low surface energy material improved the hydrophobicity of the material<sup>39</sup>.

**X-ray diffraction (XRD).** XRD analysis is most commonly used to determine the crystallinity and physical structure of the sample after the modification. Figure 7 exhibits the XRD pattern for raw and C8 treated DPF. The diffractogram of raw and C8 treated DPF shows two peaks commonly seen in DPF<sup>8,17,19</sup>. The first peak at  $16.6^\circ$  corresponding to the 101 planes represents the presence of amorphous constituents of cellulose, hemicellulose

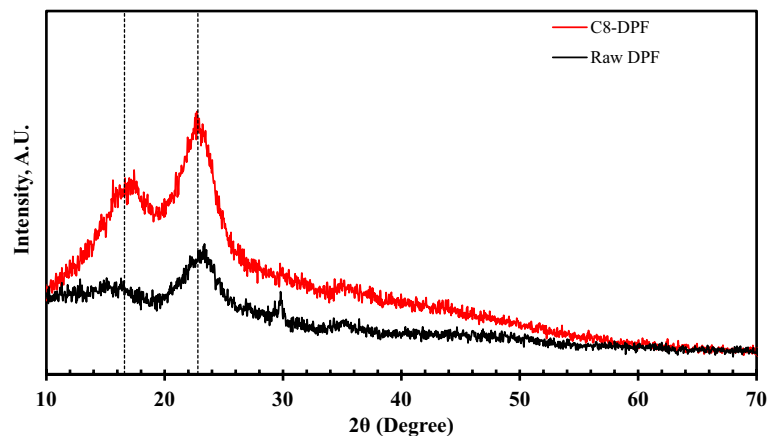


**Figure 7.** XRD patterns for raw and C8 treated DPF.

Type of sample	Crystallinity index (%)
Raw DPF	31
C8-DPF	41

**Table 1.** Crystallinity index of the raw and C8 treated DPF.

and lignin. The second peak, 23°, corresponds to the 200 plane represents the presence of  $\alpha$ -cellulose<sup>8,17,19</sup>. The experimental results reveal that during surface treatments with C8 silane, there is no structural transformation from cellulose.

Table 1 shows the crystallinity index (CI) of the raw and C8 treated DPF, calculated based on the Eq. (1). The calculated CI for the raw and C8 treated DPF was 31% and 41%, respectively. The rise in CI was observed due to the effective removal of amorphous cellulose from the fiber surface. These results are supported by the SEM micrographs, shown in Fig. 5C,D.

## Conclusions

In this research, DPF was treated with the C8 silane coupling agent and modification was able to confirm through TGA, FTIR, SEM and XRD results. With treatment of C8 thermal stability increased compared to raw DPF as per thermograms. Alkylsilane treatment can remove the non-crystalline cellulose (hemicellulose and lignin) on DPF, confirmed by decreasing mass loss of non-crystalline cellulose and increasing fiber pore size and crystallinity index, respectively, in TGA, SEM and XRD results. With the incorporation of the silane coupling agent, the hydrophilicity of the fiber converted into hydrophobic due to the lower surface energy by C8 silane coupling agent. The results indicated that alkylsilane-treated DPFs were a suitable reinforcing substitute for hydrophobic polymer composite.

## Data availability

All data generated or analysed during this study are included in this published article. The datasets used and/or analysed during the current study available from the corresponding author on reasonable request.

Received: 28 February 2022; Accepted: 25 May 2022

Published online: 13 June 2022

## References

1. Saheb, D. N. & Jog, J. P. Natural fiber polymer composites: A review. *Adv. Polym. Technol. J. Polym. Process. Inst.* **18**(4), 351–363 (1999).
2. Jain, J., Sinha, S. & Jain, S. Compendious characterization of chemically treated natural fiber from pineapple leaves for reinforcement in polymer composites. *J. Nat. Fibers* **18**(6), 845–856 (2021).
3. Nurazzi, N. M. *et al.* Treatments of natural fiber as reinforcement in polymer composites—A short review. *Funct. Compos. Struct.* **3**(2), 024002 (2021).
4. Bilba, K. & Arsene, M. A. Silane treatment of bagasse fiber for reinforcement of cementitious composites. *Compos. A Appl. Sci. Manuf.* **39**(9), 1488–1495 (2008).
5. Zahari, W. Z. W., Badri, R. N. R. L., Ardyananta, H., Kurniawan, D. & Nor, F. M. Mechanical properties and water absorption behavior of polypropylene/ijuk fiber composite by using silane treatment. *Proc. Manuf.* **2**, 573–578 (2015).
6. Harish, S., Michael, D. P., Bensely, A., Lal, D. M. & Rajadurai, A. Mechanical property evaluation of natural fiber coir composite. *Mater. Charact.* **60**(1), 44–49 (2009).
7. Karimah, A. *et al.* A review on natural fibers for development of eco-friendly bio-composite: Characteristics, and utilizations. *J. Market. Res.* **13**, 2442–2458 (2021).

8. Sathish, S. *et al.* A review of natural fiber composites: Extraction methods, chemical treatments and applications. *Mater. Today Proc.* **45**, 8017–8023 (2021).
9. Jaradat, A. & Zaid, A. Quality traits of date palm fruits in a center of origin and center of diversity. *J. Food Agric. Environ.* **2**, 208–217 (2004).
10. Turner, B. Arab organization for agricultural development (AOAD). in *The Statesman's Yearbook*. 72–72. (Palgrave Macmillan, 2008).
11. Oushabi, A. *et al.* The effect of alkali treatment on mechanical, morphological and thermal properties of date palm fibers (DPFs): Study of the interface of DPF–polyurethane composite. *S. Afr. J. Chem. Eng.* **23**, 116–123 (2017).
12. Oushabi, A. *et al.* Improvement of the interface bonding between date palm fibers and polymeric matrices using alkali-silane treatments. *Int. J. Ind. Chem.* **9**(4), 335–343 (2018).
13. Ali, M., Al-Assaf, A. H., & Salah, M. Date palm fiber-reinforced recycled polymer composites: Synthesis and characterization. *Adv. Polym. Technol.* (2022).
14. AL-Oqla, F. M., Hayajneh, M. T., & Al-Shrida, M. A. M. Mechanical performance, thermal stability and morphological analysis of date palm fiber reinforced polypropylene composites toward functional bio-products. *Cellulose*. 1–17 (2022).
15. Sanjay, M. R. *et al.* A comprehensive review of techniques for natural fibers as reinforcement in composites: Preparation, processing and characterization. *Carbohydr. Polym.* **207**, 108–121 (2019).
16. Elbadry, E. A. Agro-residues: Surface treatment and characterization of date palm tree fiber as composite reinforcement. *J. Compos.* (2014).
17. Bezazi, A., Boumediri, H., Garcia del Pino, G., Bezzazi, B., Scarpa, F., Reis, P. N., & Dufresne, A. Alkali treatment effect on physicochemical and tensile properties of date palm Rachis fibers. *J. Nat. Fibers*. 1–18 (2020).
18. Narayana, V. L. & Rao, L. B. A brief review on the effect of alkali treatment on mechanical properties of various natural fiber reinforced polymer composites. *Mater. Today Proc.* **44**, 1988–1994 (2021).
19. Perera, H. J., Goyal, A., & Alhassan, S. M. Morphological, structural and thermal properties of silane-treated date palm fibers. *J. Nat. Fibers* 1–11 (2022).
20. Xie, Y., Hill, C. A., Xiao, Z., Miltitz, H. & Mai, C. Silane coupling agents used for natural fiber/polymer composites: A review. *Compos. A Appl. Sci. Manuf.* **41**(7), 806–819 (2010).
21. Mokhothu, T. H. & John, M. J. Bio-based coatings for reducing water sorption in natural fibre reinforced composites. *Sci. Rep.* **7**(1), 1–8 (2017).
22. Meng, C. *et al.* Extraction of ramie fiber in alkali hydrogen peroxide system supported by controlled-release alkali source. *JoVE (J. Vis. Exp.)* **132**, e56461 (2018).
23. Perera, H. J., Khatiwada, B. K., Paul, A., Mortazavian, H. & Blum, F. D. Superhydrophobic surfaces with silane-treated diatomaceous earth/resin systems. *J. Appl. Polym. Sci.* **133**(41), 44072 (2016).
24. Perera, H. J., & Blum, F. D. Alkyl chain modified diatomaceous earth superhydrophobic coatings. in *2018 Advances in Science and Engineering Technology International Conferences (ASET)*. 1–4. (IEEE, 2018).
25. Perera, M. H. J. *Superhydrophobicity and Structures of Adsorbed Silane Coupling Agents on Silica and diatomaceous Earth*. Doctoral Dissertation. (Oklahoma State University, 2016).
26. Leman, Z., Zainudin, E. S., & Ishak, M. R. Effectiveness of alkali and sodium bicarbonate treatments on sugar palm fiber: Mechanical, thermal, and chemical investigations. *J. Nat. Fibers* (2018).
27. Segal, L. G. J. M. A., Creely, J. J., Martin, A. E. Jr. & Conrad, C. M. An empirical method for estimating the degree of crystallinity of native cellulose using the X-ray diffractometer. *Text. Res. J.* **29**(10), 786–794 (1959).
28. Pracella, M., Chionna, D., Anguillesi, I., Kulinski, Z. & Piorkowska, E. Functionalization, compatibilization and properties of polypropylene composites with hemp fibres. *Compos. Sci. Technol.* **66**(13), 2218–2230 (2006).
29. Kabir, M. M., Wang, H., Lau, K. T., Cardona, F. & Aravinthan, T. Mechanical properties of chemically-treated hemp fibre reinforced sandwich composites. *Compos. B Eng.* **43**(2), 159–169 (2012).
30. Sabarinathan, P., Rajkumar, K., Annamalai, V. E. & Vishal, K. Characterization on chemical and mechanical properties of silane treated fish tail palm fibres. *Int. J. Biol. Macromol.* **163**, 2457–2464 (2020).
31. Han, X. *et al.* Tuning the hydrophobicity of ZSM-5 zeolites by surface silanization using alkyltrichlorosilane. *Appl. Surf. Sci.* **257**(22), 9525–9531 (2011).
32. Atiqah, A., Jawaid, M., Ishak, M. R. & Sapuan, S. M. Effect of alkali and silane treatments on mechanical and interfacial bonding strength of sugar palm fibers with thermoplastic polyurethane. *J. Nat. Fibers* **15**(2), 251–261 (2018).
33. Zhou, F., Cheng, G. & Jiang, B. Effect of silane treatment on microstructure of sisal fibers. *Appl. Surf. Sci.* **292**, 806–812 (2014).
34. Abdelmouleh, M., Boufi, S., Belgacem, M. N., Dufresne, A. & Gandini, A. Modification of cellulose fibers with functionalized silanes: Effect of the fiber treatment on the mechanical performances of cellulose–thermoset composites. *J. Appl. Polym. Sci.* **98**(3), 974–984 (2005).
35. Yousif, B. F. & El-Tayeb, N. S. M. The effect of oil palm fibers as reinforcement on tribological performance of polyester composite. *Surf. Rev. Lett.* **14**(06), 1095–1102 (2007).
36. Chin, C. W. & Yousif, B. F. Potential of kenaf fibres as reinforcement for tribological applications. *Wear* **267**(9–10), 1550–1557 (2009).
37. Harper, P. W., Sun, L. & Hallett, S. R. A study on the influence of cohesive zone interface element strength parameters on mixed mode behaviour. *Compos. A Appl. Sci. Manuf.* **43**(4), 722–734 (2012).
38. Zhong, J., Li, H., Yu, J. & Tan, T. Effects of natural fiber surface modification on mechanical properties of poly (lactic acid)(PLA)/sweet sorghum fiber composites. *Polym.-Plast. Technol. Eng.* **50**(15), 1583–1589 (2011).
39. Abdelmouleh, M. *et al.* Modification of cellulosic fibres with functionalised silanes: Development of surface properties. *Int. J. Adhes. Adhes.* **24**(1), 43–54 (2004).

## Acknowledgements

This publication was supported by grant number [113602] from Higher Colleges of Technology (HCT). Its contents are solely the responsibility of the authors and do not necessarily represent the official views of HCT.

## Author contributions

H.P. methodology, prepared samples and wrote the main manuscript text, A.G. conducted all characterizations and S.A. provided characterization facility.

## Competing interests

The authors declare no competing interests.

## Additional information

**Correspondence** and requests for materials should be addressed to H.J.P.

**Reprints and permissions information** is available at [www.nature.com/reprints](http://www.nature.com/reprints).

**Publisher's note** Springer Nature remains neutral with regard to jurisdictional claims in published maps and institutional affiliations.



**Open Access** This article is licensed under a Creative Commons Attribution 4.0 International License, which permits use, sharing, adaptation, distribution and reproduction in any medium or format, as long as you give appropriate credit to the original author(s) and the source, provide a link to the Creative Commons licence, and indicate if changes were made. The images or other third party material in this article are included in the article's Creative Commons licence, unless indicated otherwise in a credit line to the material. If material is not included in the article's Creative Commons licence and your intended use is not permitted by statutory regulation or exceeds the permitted use, you will need to obtain permission directly from the copyright holder. To view a copy of this licence, visit <http://creativecommons.org/licenses/by/4.0/>.

© The Author(s) 2022